Journal of the American College of Cardiology
© 2004 by the American College of Cardiology Foundation
Published by Elsevier Inc.

Vol. 44, No. 7, 2004
ISSN 0735-1097/04/$30.00
doi:10.1016/j.jacc.2004.05.083

PRECLINICAL RESEARCH

Effect of Granulocyte-Macrophage Colony-Stimulating Factor Inducer on Left Ventricular Remodeling After Acute Myocardial Infarction

Yuichiro Maekawa, MD, Toshihisa Anzai, MD, Tsutomu Yoshikawa, MD, Yasuo Sugano, MD, Keitaro Mahara, MD, Takashi Kohno, MD, Toshiyuki Takahashi, MD, Satoshi Ogawa, MD, FACC
Tokyo, Japan

OBJECTIVES We sought to determine the influence of granulocyte-macrophage colony-stimulating factor (GM-CSF) induction on post-myocardial infarction (MI) remodeling, especially in relation to the inflammatory response and myocardial fibrosis.

BACKGROUND Granulocyte-macrophage colony-stimulating factor modifies wound healing by promoting monocytopoiesis and infiltration of monocytes and macrophages into injured tissue; however, the effect of GM-CSF induction on the infarct healing process and myocardial fibrosis is unclear.

METHODS A model of MI was produced in Wistar rats by ligation of the left coronary artery. The MI animals were randomized to receive GM-CSF inducer (romurtide 200 μg/kg/day for 7 consecutive days) (MI/Ro) or saline (MI/C).

RESULTS Echocardiographic and hemodynamic studies on day 14 revealed increased left ventricular (LV) end-diastolic dimension, decreased fractional shortening, elevated LV end-diastolic pressure, and decreased LV maximum rate of isovolumic pressure development in MI/Ro compared with MI/C. Immunoblotting showed that expression of transforming growth factor (TGF)-β1 in the infarcted site on day 3 after MI was decreased in MI/Ro compared with MI/C. In the infarcted site, TGF-β1, collagen type I and type III messenger ribonucleic acid (mRNA) expression on day 3, and collagen content on day 7 were reduced in MI/Ro compared with MI/C, in association with marked infarct expansion. In MI/Ro, monocyte chemoattractant protein-1 mRNA level and the degree of infiltration of monocyte-derived macrophages (ED-1-positive) were greater in the infarcted site on day 7 than those in MI/C.

CONCLUSIONS The GM-CSF induction by romurtide facilitated infarct expansion in association with the promotion of monocyte recruitment and inappropriate collagen synthesis in the infarcted region during the early phase of MI. (J Am Coll Cardiol 2004;44:1510–20) © 2004 by the American College of Cardiology Foundation

Congestive heart failure is the most common cause of cardiac death after myocardial infarction (MI) and develops during the process of left ventricular (LV) remodeling, which consists of infarct expansion followed by progressive dilation (1). Defective infarct healing, infarct size, and wall

See page 1521

stress, are major determinants of infarct expansion (2). In the initial stages of infarct healing, peripheral monocytes infiltrate the necrotic myocardium through the up-regulation of monocyte chemoattractant protein (MCP)-1, and they differentiate into macrophages. These monocytes and macrophages produce transforming growth factor (TGF)-β1, which is a fibrogenic cytokine related to collagen accumulation. Appropriate collagen deposition in the infarcted site is necessary to prevent infarct expansion caused by wall stress. Monocytes and macrophages orchestrate the infarct healing process through a complex cascade involving cytokines, growth factors, and collagen turnover.

Granulocyte-macrophage colony-stimulating factor (GM-CSF) is a cytokine that stimulates the growth and differentiation of granulocyte and macrophage precursor cells in vitro (3). The GM-CSF induces peripheral monocytosis and prolongs the life-span of monocytes via a reduction of apoptosis. It has been reported that peripheral monocytosis is associated with LV remodeling after MI (4). Another study demonstrated that plasma GM-CSF levels were elevated in patients with ischemic dilated cardiomyopathy and that this increase was associated with the degree of LV dysfunction (5). Romurtide, which is a synthetic muramyldipeptide derivative, has been known to act as a GM-CSF inducer by binding to monocytes and macrophages (6,7). The aim of this study

From the Division of Cardiology, Department of Medicine, Keio University School of Medicine, Tokyo, Japan. Supported in part by grants for scientific research 14770333 (Dr. Maekawa) and 14570693 (Dr. Anzai) from the Ministry of Education, Science, and Culture of Japan.

Manuscript received January 27, 2004; revised manuscript received April 12, 2004, accepted May 19, 2004.

Abbreviations and Acronyms

ECM = extracellular collagen matrix
GAPDH = glyceraldehyde 3-phosphate dehydrogenase
GM-CSF = granulocyte-macrophage colony-stimulating factor
LV = left ventricular/ventricle
LVEDD = left ventricular end-diastolic dimension
LVESD = left ventricular end-systolic dimension
MCP = monocyte chemoattractant protein
MI = myocardial infarction
mRNA = messenger ribonucleic acid
PCR = polymerase chain reaction
RWT = relative wall thickness
TGF = transforming growth factor

was to determine the influence of GM-CSF induction on post-MI remodeling, especially in relationship to the infarct healing process and myocardial fibrosis.

METHODS

Experimental animals. All experiments were performed in accordance with the protocols approved by the Institutional Animal Care and Use Committee. Male Wistar rats weighing 250 to 300 g were used. All rats were housed under identical conditions and given food and water ad libitum.

Experimental protocol. The rats were anesthetized with an intraperitoneal injection (IP) of sodium pentobarbital (50 mg/kg), intubated, and ventilated with a volume-cycled small-animal respirator. The heart was exposed through a left thoracotomy, and MI was induced by ligating the left coronary artery with a prolene 6-0 suture. Rats that died within 24 h after the operation were excluded from the analysis. The sham-operated animals underwent the same procedure without ligation of the coronary artery and received an IP of saline (Sham) or 200 μg/kg/day of GM-CSF inducer (romurtide) for seven days (Sham/Ro). The MI rats were also treated with saline (MI/C) or a 200 μg/kg/day IP of romurtide for seven days (MI/Ro). We determined the dosage of romurtide based on results demonstrated by the dosage used to obtain GM-CSF induction in previous studies. The rats were assigned to four groups (Sham, Sham/Ro, MI/C, and MI/Ro). The investigators were blinded regarding sham versus MI and saline versus romurtide. The heart was excised under an IP of sodium pentobarbital at 3, 7, or 14 days after surgery for each group. The LV was separated from the atria and the right ventricle, and each was weighed, immediately frozen in liquid nitrogen, and stored at −80°C until use.

Hemodynamic measurements. On day 14, hemodynamic parameters were measured in the lightly anesthetized rats (sodium pentobarbital IP). The right carotid artery was cannulated with a Millar ultraminiature catheter (SPR-671, 1.4-F, Millar Instruments, Houston, Texas) and advanced into the aorta to record arterial pressure. The aortic catheter was then advanced into the LV to record pressure, the maximum rate of isovolumic pressure development ($+dP/dt_{max}$), and the minimum rate of isovolumic pressure decay ($-dP/dt_{min}$).

Echocardiographic study. Transthoracic echocardiographic studies were performed on the lightly anesthetized rats on day 14 using an echocardiographic system equipped with a 12-MHz phased-array transducer (Envisor M2540, Philips Medical Systems, Andover, Massachusetts). M-mode tracings were recorded through the anterior and posterior LV walls at the papillary muscle level to measure left ventricular end-diastolic dimension (LVEDD), left ventricular end-systolic dimension (LVESD), and LV anterior and posterior wall thickness at end-diastole. The LV fractional shortening and relative wall thickness (RWT) were calculated according to the following formulas: LV fractional shortening = [(LVEDD − LVESD)/LVEDD] × 100; RWT = 2 × posterior wall thickness at end-diastole/LVEDD.

Infarct size. After taking the hemodynamic and echocardiographic recordings, the LV was fixed by immersion in 10% formalin and embedded in paraffin. Six transverse slices were cut from the apex to the base, and serial sections were cut and mounted. The percentage of infarcted LV was estimated on day 14 using planimetric techniques (8). Specimens with a large infarct (>40% of the LV free wall) were used in this study.

Expansion index. The expansion index was determined on day 14 using 10% paraformaldehyde-fixed tissue as previously described (9). The expansion index was calculated with the following formula: expansion index = (LV cavity area/total LV area) × (septal thickness/scar thickness).

Peripheral leukocyte count. Approximately 1 ml of peripheral blood was drawn from each rat on days 1, 2, 4, and 7 for measuring leukocyte counts. The total leukocyte count was obtained using an improved Neubauer chamber, and the proportion of monocytes was determined using Giemsa-stained blood smears.

Western blotting. Frozen tissue was homogenized in buffer containing protease inhibitors in phosphate-buffered saline. Equal amounts of the denatured protein were then analyzed using sodium dodecyl sulfate-polyacrylamide gel electrophoresis. The TGF-β1 protein was probed with a rabbit polyclonal antibody (1:500 dilution, Santa Cruz Biotechnology Inc., Santa Cruz, California). Horseradish peroxidase-conjugated sheep anti-rabbit immunoglobulin G (1:5,000 dilution, Roche Molecular Biochemicals, Indianapolis, Indiana) was used as the secondary antibody. The reaction was developed using enhanced chemiluminescence reagents (Amersham Biosciences, Piscataway, New Jersey), and an image was obtained by exposure to X-ray film. Densitometric quantification was then performed using Scion image software (Scion Corporation, Frederick, Maryland). The results were presented as a percentage by comparing them with those of an untreated control, and the control mean was arbitrarily set as 100%.

Ribonucleic acid preparation. Total cellular ribonucleic acid was isolated using a modification of the acid guanidium thiocyanate and phenol/chloroform extraction method, and

using TRIzol LS Reagent (Life Technologies, Rockville, Maryland) according to the manufacturer's protocol.

TaqMan real-time reverse transcription polymerase chain reaction analysis. The expression of MCP-1, TGF-β1, collagen type I and type III, GM-CSF, and glyceraldehyde 3-phosphate dehydrogenase (GAPDH) messenger ribonucleic acid (mRNA) was studied using quantitative real-time reverse transcription polymerase chain reaction (PCR). The TaqMan probes were labeled with a 5′ reporter dye, 6-carboxyfluorescein and a 3′ quencher dye, 6-carboxyltetramethyl-rhodamine. During the PCR reaction, the AmpliTaq Gold DNA polymerase cleaves the TaqMan probe at the 5′ end and separates the reporter dye from the quencher dye if the probe hybridizes to the target. This cleavage results in the generation of a fluorescent signal by the cleaved reporter dye, which is directly monitored by the ABI Prism 7700 Detection System (Perkin-Elmer Corp., Foster City, California). The PCR conditions were as follows: 45 cycles of denaturing at 95°C for 15 s and primer annealing/extension at 60°C for 60 s. The increase in fluorescent signal is proportional to the amount of specific PCR product generated. Primers and probes used for MCP-1, TGF-β1, collagen type I and type III, GM-CSF, and GAPDH were as follows: MCP-1, forward primer: 5′-CTCAGCCAGATGCAGTTAATGC-3′; reverse primer: 5′-TTCTCCAGCCGACTCATTGG-3′; TaqMan probe: 5′-TCACCTGCTGCTACTCATTCACTGGC-3′; TGF-β1, forward primer: 5′-GGCACCATCCATGACATGAA-3′; reverse primer: 5′-CAGGTGTTGAGCCCTTTCCA-3′; TaqMan probe: 5′-CCTTCCTGCTCCTCATGGCCACC-3′; collagen type I, forward primer: 5′-CCAGTTCGAGTATGGAAGCGA-3′; reverse primer: 5′-AGGTGATGTTCTGGG-3′; TaqMan probe: 5′-CCTGCGCCTGATGTCCACCGA-3′; collagen type III, forward primer: 5′-CAGCTGGCCTTCCTCAGACTT-3′; reverse primer: 5′-GCTGTTTTTGCAGTGGTATGTAATGT-3′; TaqMan probe: 5′-TTTCCAGCCGGGCCTCCCAG-3′; GM-CSF, forward primer: 5′-AGACCCGCCTGAAGCTATACAA-3′; reverse primer: 5′-CTGGTAGTGGCTGGCTATCATG-3′; TaqMan probe: 5′-CCTCACCAAACTCAATGGCGCCTTG-3′; GAPDH, forward primer: 5′-AACTCCCTCAAGATTGTCAGCAA-3′; reverse primer: 5′-GTGGTCATGAGCCCTTCCA-3′; TaqMan probe: 5′-CTGCACCACCAACTGCTTAGCCCC-3′. Data were analyzed using a Sequence Detector V1.6 program (Perkin-Elmer). The obtained CT (cycle number at which an amplification threshold of detection is reached) values were normalized to rodent GAPDH expression by the $\Delta\Delta$Ct method using trough sham levels as the calibrator value (10).

Determination of collagen concentration. Tissue homogenates were freeze-dried, weighed, and hydrolyzed in 6N hydrochloric acid at 110°C for 24 h. Hydroxyproline concentration was measured spectrophotometrically (11). Collagen content was expressed in μg/mg dry tissue weight assuming that collagen contains an average of 13.4% hydroxyproline. Assays were performed in duplicate.

Immunohistochemical evaluation. For immunohistochemical evaluation, immunoperoxidase methods were employed. The excised heart was fixed with 10% paraformaldehyde and embedded in paraffin according to routine procedures. The paraffin-embedded specimen was then cut into 6-μm-thick sections and mounted on silanized slides. Sections were deparaffinized in xylene and dehydrated through a graded series of ethanol concentrations. Endogenous peroxidase activity was blocked by 3% hydrogen peroxide for 5 min. The sections were then incubated with a primary antibody, ED-1 (Serotec, Oxford, United Kingdom) at a dilution of 1:50 for 60 min at room temperature or MCP-1 (Cedarlane, Ontario, Canada) at a dilution of 1:100 for overnight at 4°C. Next, the sections were treated with a biotinylated secondary antibody, anti-rabbit immunoglobulin G serum, for 10 min at room temperature using an LSAB2 kit (Dako, Carpinteria, California). After being washed for 10 min in phosphate-buffered saline, the sections were incubated with streptavidin peroxidase for 10 min. The sections were then washed again for 10 min in phosphate-buffered saline and finally, colored with 3-amino-9-ethylcarbazole in *N*-dimethylformamidine. Serial sections were stained with hematoxylin-eosin.

Quantitative histologic analysis. Stained sections were photographed with a Nikon digital camera (Nikon Corp., Tokyo, Japan) mounted on an Olympus microscope (Olympus Corp., Tokyo, Japan). Multiple digital images were taken and stored for each sample. Staining was quantitatively analyzed using Scion image software (Scion Corp). The number of macrophages was quantified by counting the total number of positively stained ED-1 cells in 20 grid fields with a total area of 0.1 mm^2. Four animals from each group were used for quantitation.

Statistical analyses. All values are presented as mean ± SEM. One-way analysis of variance was performed for statistical comparisons, and if the analysis of variance results were significant, Scheffé's post hoc test was performed. Two-way repeated measures analysis of variance followed by Scheffé's post hoc test was performed for analysis of the time-course variations. Significance was taken as $p < 0.05$. All statistical analyses were performed using Statview 5.0 software (SAS Institute Inc., Cary, North Carolina).

RESULTS

Mortality. Coronary artery ligation was performed in 105 rats. The perioperative mortality rate, within 24 h after the operation, was 43% (45 rats). Finally, 60 rats were randomly allocated to four groups as follows: Sham (13 rats), Sham/Ro (13 rats), MI/C (17 rats), and MI/Ro (17 rats). The mortality of MI/Ro rats (8 deaths [47%]) was higher than that of MI/C rats (4 deaths [24%]; $p < 0.05$). In sham-operated rats, romurtide administration had no effect on mortality (Sham vs. Sham/Ro, 1 death [8%] vs. 1 death

Table 1. Physiologic, Hemodynamic, and Echocardiographic Parameters on Day 14

	Sham (n = 6)	Sham/Ro (n = 5)	MI/C (n = 6)	MI/Ro (n = 5)
BW (g)	296 ± 10	300 ± 25	295 ± 15	297 ± 13
RV/BW (g/kg)	0.7 ± 0.1	0.7 ± 0.1	0.6 ± 0.2	0.7 ± 0.1
LV/BW (g/kg)	2.3 ± 0.1	2.3 ± 0.1	2.4 ± 0.2	2.4 ± 0.1
LVSP (mm Hg)	133 ± 12	125 ± 10	115 ± 17	118 ± 7
LVEDP (mm Hg)	5 ± 1	6 ± 1	8 ± 2	13 ± 2*†‡
LV $+dP/dt_{max}$ (mm Hg/s)	5,222 ± 236	5,002 ± 221	4,523 ± 236*†	3,680 ± 211*†‡
LV $-dP/dt_{min}$ (mm Hg/s)	5,422 ± 215	5,312 ± 241	4,232 ± 255*†	3,920 ± 210*†
LVEDD (mm)	5.5 ± 0.4	6.1 ± 0.5	6.7 ± 0.3*	8.0 ± 0.4*†‡
LVESD (mm)	3.3 ± 0.2	3.9 ± 0.3	5.2 ± 0.2*†	6.4 ± 0.3*†‡
FS (%)	39 ± 1	37 ± 1	24 ± 6*†	18 ± 3*†‡
RWT	0.5 ± 0.1	0.4 ± 0.1	0.4 ± 0.1	0.3 ± 0.1

Values are mean ± SEM. *p < 0.05 versus Sham; †p < 0.05 versus Sham/Ro; ‡p < 0.05 versus MI/C.

BW = body weight; FS = fractional shortening; LV = left ventricular; LVEDD = left ventricular end-diastolic dimension; LVEDP = left ventricular end-diastolic pressure; LVESD = left ventricular end-systolic dimension; LV $+dP/dt_{max}$ = left ventricular maximum rate of isovolumic pressure development; LV $-dP/dt_{min}$ = left ventricular minimum rate of isovolumic pressure decay; LVSP = left ventricular systolic pressure; MI/C = myocardial infarction rats treated with saline; MI/Ro = MI treated with romurtide; RV = right ventricular; RWT = relative wall thickness; Sham = sham-operated rats treated with saline; Sham/Ro = Sham treated with romurtide.

[8%], p = NS). No deaths involved cardiac rupture in all groups.

Physiologic, hemodynamic, and echocardiographic parameters. The body weight of MI/Ro was not significantly increased compared with those of the sham-operated control and MI/C groups. The heart weight to body weight ratio was similar among the four groups. The LV end-diastolic pressure in MI/Ro was significantly higher than that in MI/C. The LV $+dP/dt_{max}$ in MI/Ro was significantly lower than that in MI/C. In sham-operated rats, romurtide treatment had no effect on any of the hemodynamic variables measured. The LVEDD and LVESD in MI/Ro were increased compared with those in MI/C. The fractional shortening was significantly decreased in MI/Ro compared with MI/C. The RWT was similar among the four groups (Table 1).

Infarct expansion on histologic analysis. Infarct expansion was more apparent on histologic analysis in MI/Ro

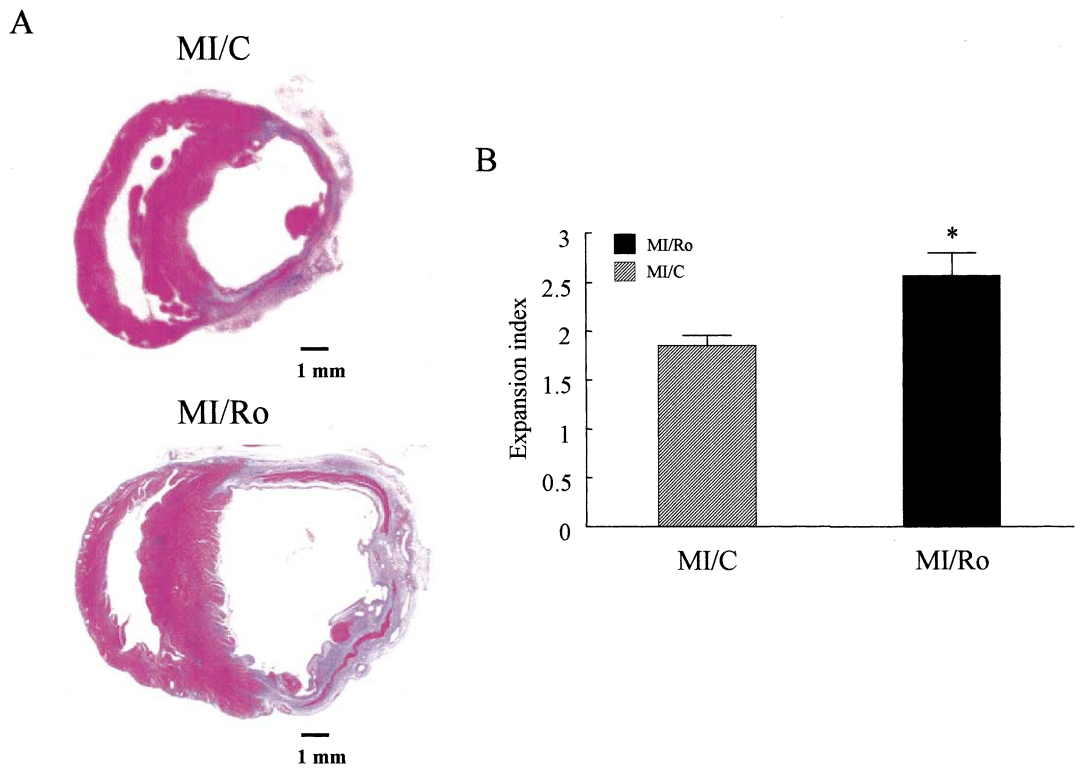

Figure 1. (A) Representative hematoxylin-eosin-stained midventricular cross-sections of myocardial infarction rats treated with saline (MI/C) and myocardial infarction treated with romurtide (MI/Ro) on day 14. **(B)** Expansion index on day 14 in MI/C and MI/Ro (n = 4 per group). Values are mean ± SEM. *p < 0.05 versus MI/C.

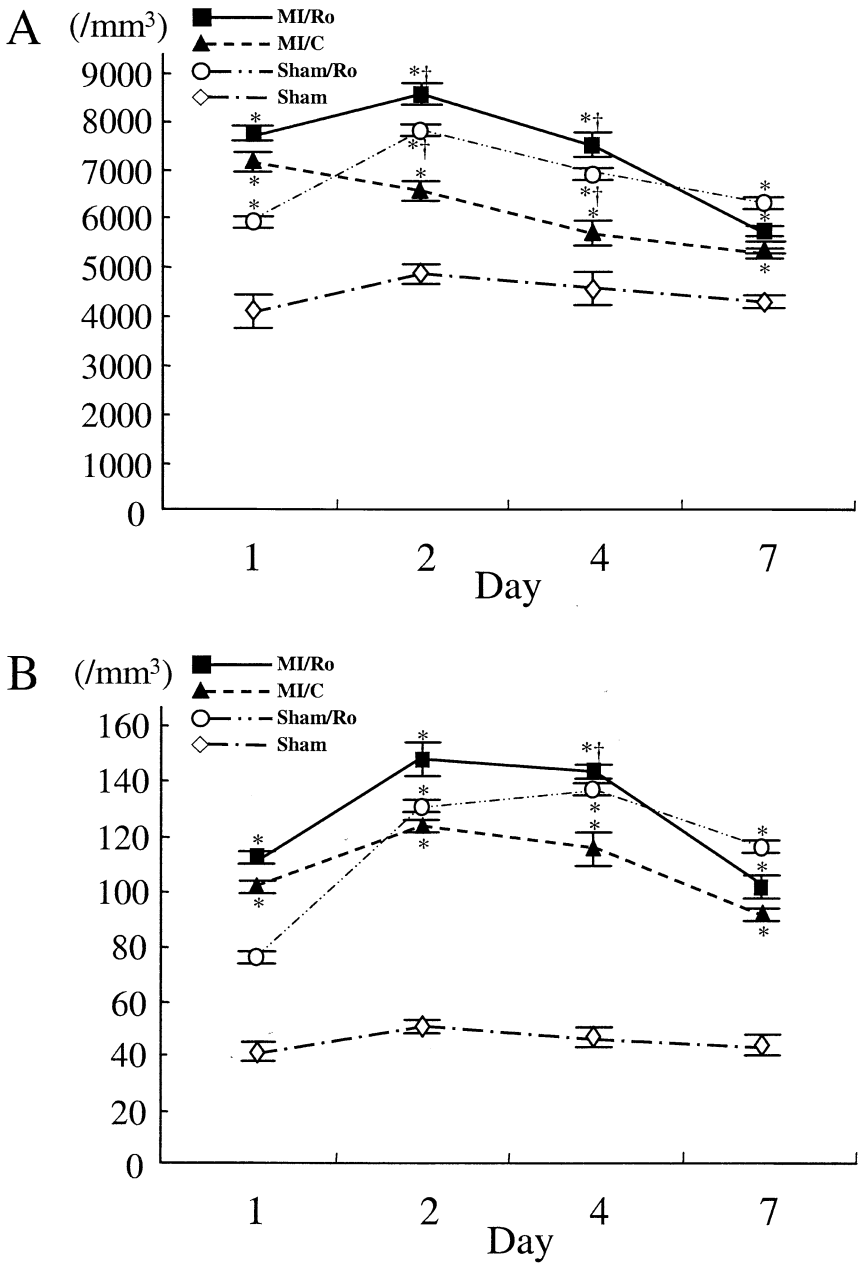

Figure 2. **(A)** Time course difference of peripheral leukocyte count among sham-operated rats (Sham), Sham treated with romurtide (Sham/Ro), myocardial infarction rats treated with saline (MI/C), and myocardial infarction treated with romurtide (MI/Ro) (n = 4 per group). **(B)** Time course difference of peripheral monocyte count among Sham, Sham/Ro, MI/C, and MI/Ro (n = 4 per group). Values are mean ± SEM. *$p < 0.05$ versus Sham; †$p < 0.05$ versus MI/C.

compared with MI/C (Fig. 1A). Expansion index in MI/Ro was higher than that in MI/C (Fig. 1B).

Changes of peripheral leukocyte and monocyte count. Peripheral leukocyte counts in Sham/Ro and MI/Ro on days 2 and 4 were significantly increased compared with those in MI/C (Fig. 2A). Peripheral monocyte count in MI/Ro on day 4 was significantly increased compared with that in MI/C (Fig. 2B).

Induction of local GM-CSF expression. The GM-CSF mRNA expression was increased 1.5-fold on day 3 ($p < 0.05$) and 2-fold on day 7 ($p < 0.05$) in the infarcted myocardium of MI/C as compared with the LV of Sham. The GM-CSF mRNA expression was increased 2.3-fold on day 3 ($p < 0.05$) and 2-fold on day 7 ($p < 0.05$) in the infarcted myocardium of MI/Ro as compared with MI/C. However, myocardial GM-CSF expression was not increased by romurtide treatment in sham-operated rats. In the non-infarcted sites of MI rats and in the myocardium of sham rats, GM-CSF expression was not different during the whole-examined period.

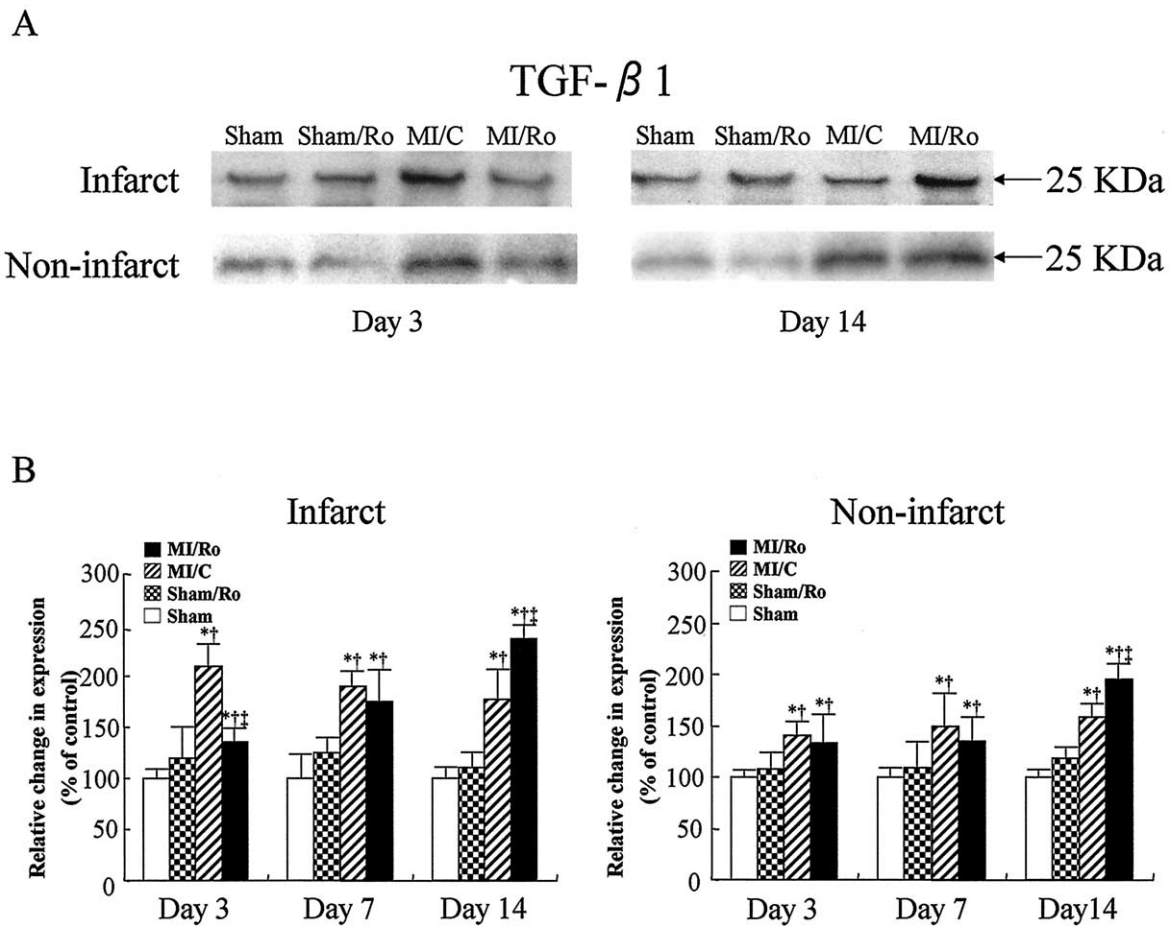

Figure 3. (A) Representative immunoblots showing transforming growth factor (TGF)-β1 protein level in the infarcted and non-infarcted sites on days 3 and 14 among sham-operated rats (Sham), Sham treated with romurtide (Sham/Ro), myocardial infarction rats treated with saline (MI/C), and MI treated with romurtide (MI/Ro). **(B)** Quantified data of TGF-β1 protein expression in the infarcted and non-infarcted sites among Sham, Sham/Ro, MI/C, and MI/Ro (n = 4 per group). Values are mean ± SEM. *p < 0.05 versus Sham; †p < 0.05 versus Sham/Ro; ‡p < 0.05 versus MI/C.

Effect of GM-CSF inducer on MCP-1, TGF-β1, collagen type I and type III expression. Figure 3 shows the serial changes in myocardial protein expression of TGF-β1. The TGF-β1 protein in the infarcted site on day 3 was decreased in MI/Ro compared with MI/C. However, the increase of TGF-β1 protein in MI/Ro was more prominent on day 14 compared with that in MI/C. The TGF-β1 protein expression in the non-infarcted site was also increased in MI/Ro compared with MI/C on day 14.

Serial changes in mRNA expression of these parameters are shown in Figure 4. In the infarcted myocardium, TGF-β1, collagen type I and type III mRNA expression on day 3 were decreased in MI/Ro compared with MI/C. The MCP-1 mRNA expression in the infarcted site on days 3 and 7 was enhanced in MI/Ro compared with MI/C. The TGF-β1, collagen type I and type III mRNA expression in the infarcted and non-infarcted areas on day 14 was increased by romurtide treatment.

Inflammatory and fibrotic changes in histologic and immunohistologic analyses. On day 7, ED-1-positive macrophages massively infiltrated the infarcted site in MI/Ro compared with MI/C. There were significantly increased numbers of ED-1-positive macrophages in the infarct zone (MI/Ro, 1,320 ± 145 cells/mm^2 vs. MI/C, 686 ± 125 cells/mm^2, $p < 0.05$). The MCP-1-positive cells in the infarcted site were also more prominent in MI/Ro than in MI/C (MI/Ro, 420 ± 151 cells/mm^2 vs. MI/C, 235 ± 105 cells/mm^2, $p < 0.05$). These were not observed in the myocardium of Sham and Sham/Ro (Fig. 5A). Mallory-Azan staining showed that fibrosis in the infarcted site was attenuated on day 7 but augmented on day 14 by romurtide treatment (Fig. 5B).

Collagen concentration. In the infarcted region of romurtide-treated MI rats, collagen content, assessed by hydroxyproline concentration, was significantly lower on day 7 but higher on day 14 compared with MI/C. Collagen content in the non-infarcted region of the romurtide-treated MI rats was significantly increased on day 14 compared with MI/C (Fig. 5C).

DISCUSSION

The GM-CSF induction by romurtide increased the peripheral monocyte count, expression of MCP-1 mRNA,

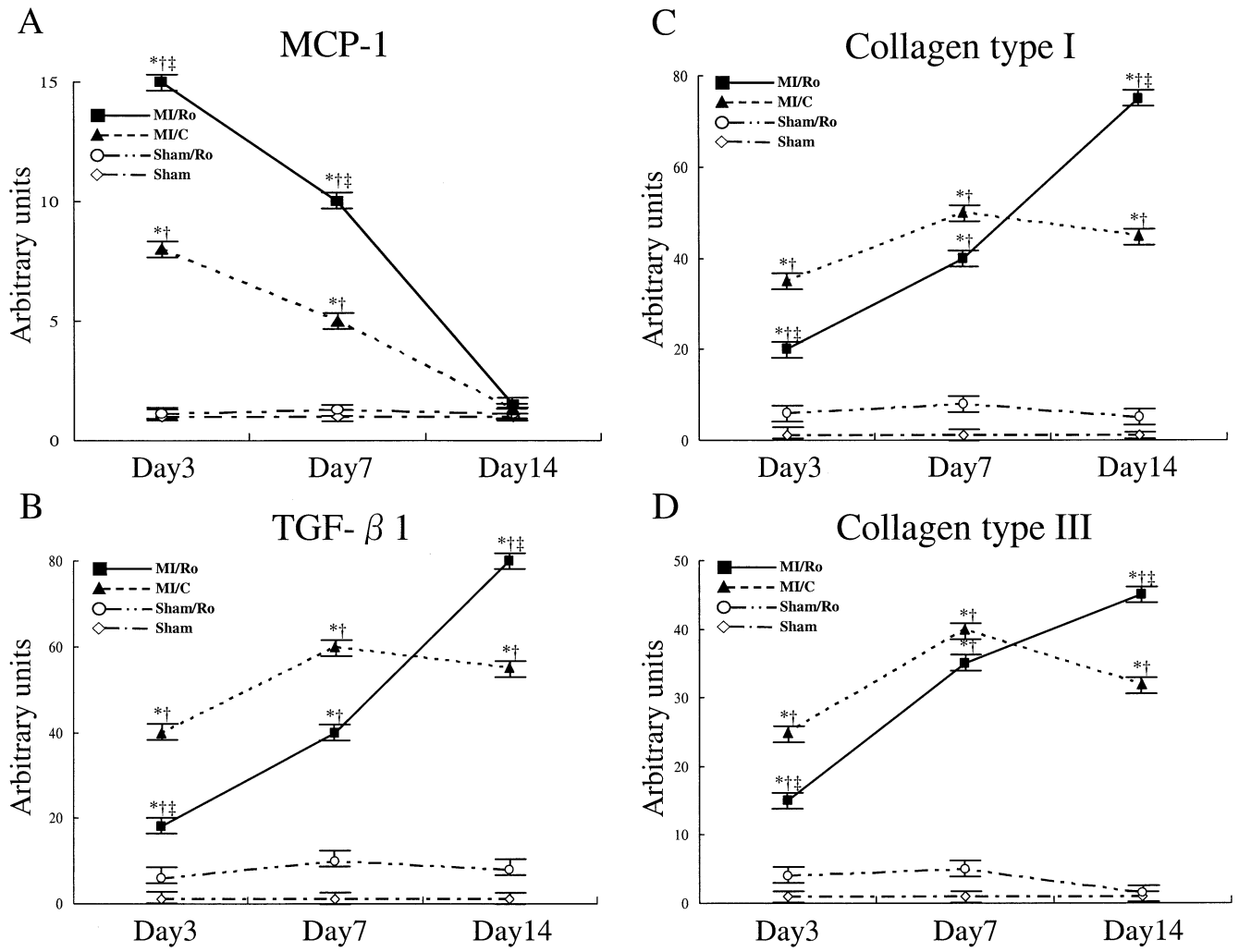

Figure 4. Effects of romurtide administration on monocyte chemoattractant protein (MCP)-1, transforming growth factor (TGF)-β1, and collagen type I and collagen type III messenger ribonucleic acid (mRNA) expression in the infarcted and non-infarcted sites. Quantitative analyses showing **(A)** MCP-1, **(B)** TGF-β1, **(C)** collagen type I, and **(D)** collagen type III mRNA expression in the infarcted sites and **(E)** MCP-1, **(F)** TGF-β1, **(G)** collagen type I, and **(H)** collagen type III mRNA expression in the non-infarcted sites with real-time reverse transcription polymerase chain reaction analyses among sham-operated rats (Sham), Sham treated with romurtide (Sham/Ro), myocardial infarction rats treated with saline (MI/C), and MI treated with romurtide (MI/Ro) (n = 5 per group). Values are mean ± SEM. *p < 0.05 versus Sham; †p < 0.05 versus Sham/Ro; ‡p < 0.05 versus MI/C. *Continued on next page.*

and infiltration of ED-1-positive macrophages and reduced the expression of TGF-β1, collagen type I and type III mRNA in the infarcted myocardium during the early phase of MI. Peripheral monocytosis, enhanced monocyte recruitment into the infarcted myocardium, and delayed collagen production by GM-CSF induction resulted in infarct expansion and aggravated LV remodeling.

Previous studies have demonstrated that excessive infiltration of leukocytes might be harmful for tissue repair. In secretory leukocyte protease inhibitor-deficient mice, exaggerated leukocyte infiltration into wound sites was associated with impaired wound healing (12). Alternatively, reduction of leukocyte infiltration in tumor necrosis factor receptor p55-deficient mice resulted in accelerated wound healing (13). Because GM-CSF delays macrophage and monocyte apoptosis (14,15), it is possible that the enhanced and persistent infiltration of macrophages induced by romurtide administration might cause delayed infarct healing.

In our study, romurtide treatment promoted ED-1-positive macrophages infiltration in the infarcted myocardium of MI rats but not in the myocardium of sham-operated rats, despite a similar increase in peripheral monocyte count. Many studies have demonstrated that GM-CSF promotes the infiltration of monocytes and macrophages after tissue injury. However, GM-CSF itself has no effect on monocyte transmigration or adhesion to cultured endothelial cells (14). Under the influence of chemoattractants such as MCP-1 that are produced in response to injury, GM-CSF promotes the effective recruitment of circulating monocytes to local inflammatory sites by attachment to the endothelium (16,17).

Collagen deposition plays a role in preserving ventricular

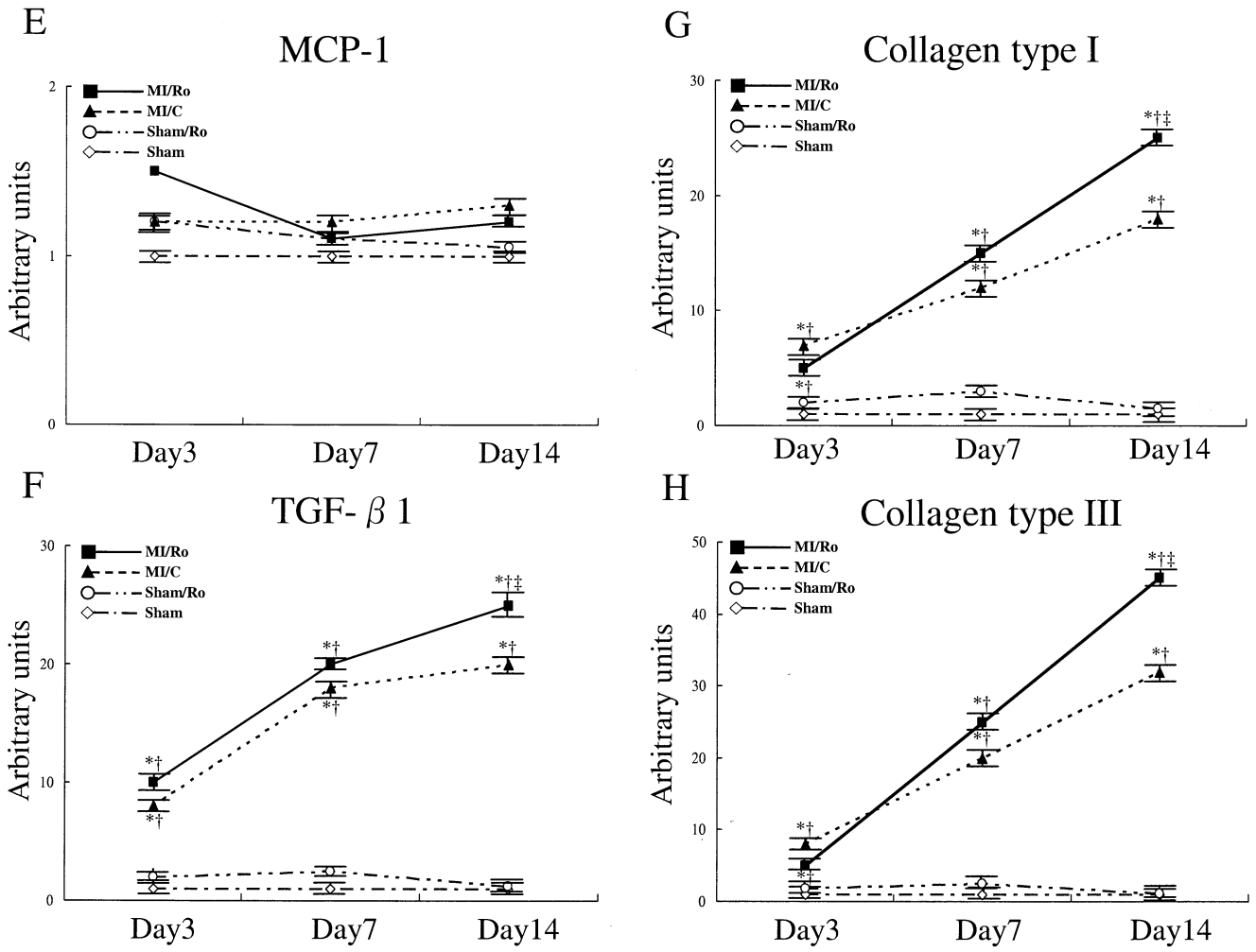

Figure 4 Continued.

structure and function. In an experimental model, inhibition of collagen accumulation, which was induced by osteopontin knock-out, caused excessive infarct expansion during the infarct healing process (18). In human experimental wounds, GM-CSF inhibited collagen deposition, possibly through prolonged monocyte infiltration (19). In the present study, romurtide induced peripheral monocytosis, MCP-1 upregulation, and ED-1-positive macrophage infiltration, suggesting excessive inflammation in local infarcted sites. Additionally, collagen production in the infarcted site was inhibited by romurtide administration during the early phase of MI. These results indicate that prolonged inflammation might delay collagen production, resulting in infarct expansion. Although an earlier study demonstrated that collagen type I and type III mRNA expression levels reached a peak at seven days after MI in the rat heart (20), the mRNA levels on day 14 were even higher than those on day 7 in romurtide-treated MI rats in our study.

Degradation of extracellular collagen matrix (ECM) also plays an important role in post-MI remodeling. Several proteinases, including matrix metalloproteinases, plasmin, and cathepsin are expressed in the infiltrating inflammatory cells in the infarcted area (21,22). These enzymes are known to be related to the occurrence of cardiac rupture and LV remodeling. Previous studies showed that the incidence of cardiac rupture in a mouse MI model was reduced by knock-out of matrix metalloproteinase-9, urokinase-type plasminogen activator, or plasminogen in association with less leukocyte infiltration into the infarcted area (23,24). In our study, on day 7, collagen content was lower and the infiltration of ED-1-positive macrophages was more prominent in the infarcted area of romurtide-treated MI rats than that of MI-control rats. These findings demonstrated that excessive infiltration of inflammatory cells might cause an imbalance of ECM synthesis/degradation, resulting in adverse post-MI remodeling.

Myofibroblasts are important for fibrogenesis at sites of remodeling after MI. Transforming growth factor-β1 is a major fibrogenic cytokine and contributes to differentiation of fibroblasts into myofibroblasts. Myofibroblasts are colocalized with accumulated collagen and are responsible for increased expression of collagen type I and type III. The TGF-β1 in the infarcted myocardium is primarily produced

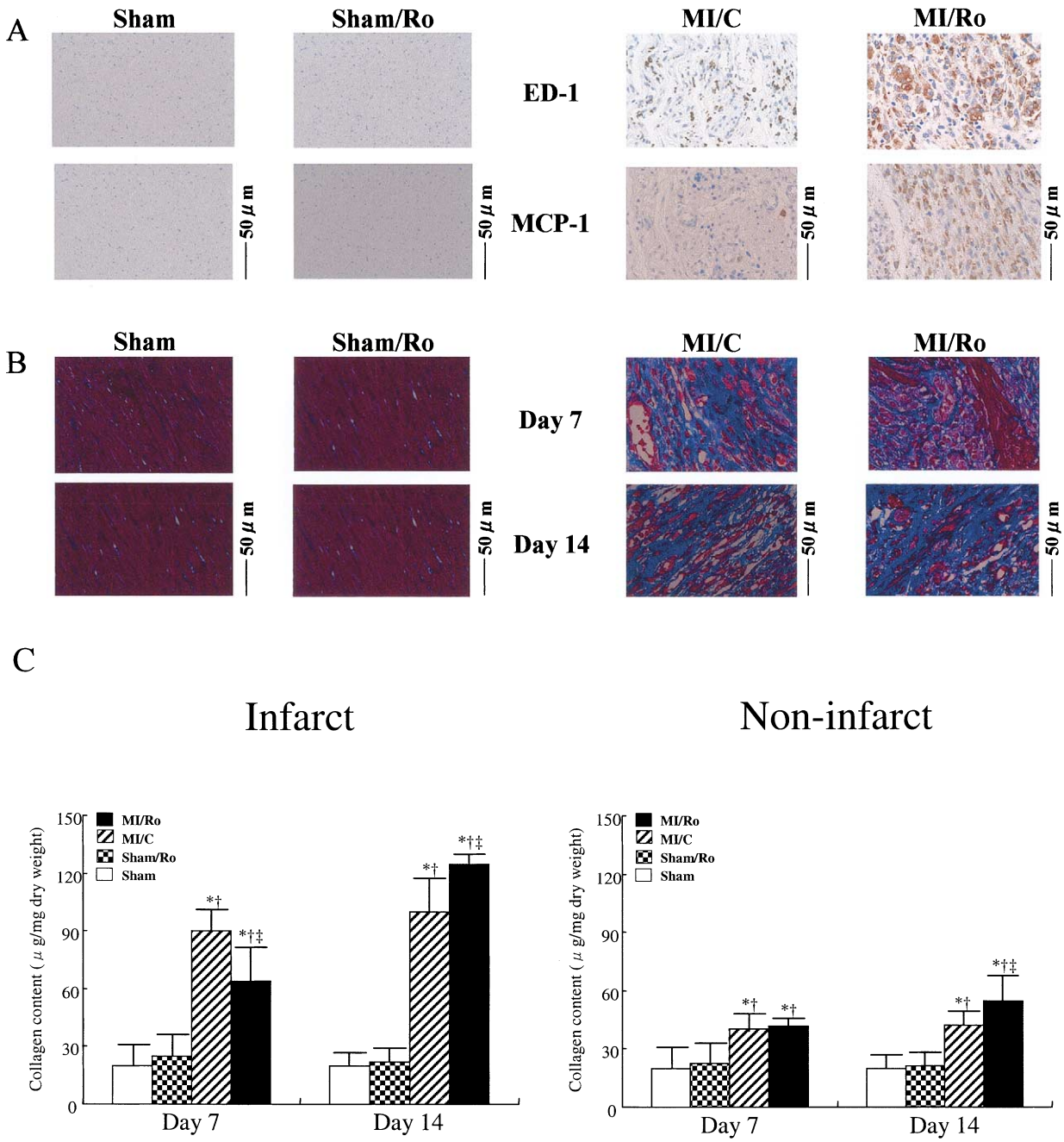

Figure 5. **(A)** Results of immunohistochemical staining of the infarcted sites of the myocardial infarction rats treated with saline (MI/C) and MI treated with romurtide (MI/Ro), and of the left ventricle (LV) of the sham-operated rats (Sham) and Sham treated with romurtide (Sham/Ro) on day 7 with use of monoclonal anti-ED-1 and anti-monocyte chemoattractant protein-1 (anti-MCP-1) antibodies (magnification 400×). The ED-1-positive macrophages and MCP-1-positive cells are stained brown. **(B)** Mallory-Azan staining in the infarcted sites of the MI animals (MI/C and MI/Ro) and in the LV of the sham animals (Sham and Sham/Ro) on days 7 and 14 (magnification 400×). Fibrous tissue appears blue. **(C)** Collagen content in the infarcted and non-infarcted sites of MI/C and MI/Ro and in the LV of Sham and Sham/Ro (n = 4 per group). Values are mean ± SEM. *p < 0.05 versus Sham; †p < 0.05 versus Sham/Ro; ‡p < 0.05 versus MI/C.

by macrophages in the early phase of repair and myofibroblasts in the fibrogenic phase of healing (25). It is possible that prolonged activation of macrophages by GM-CSF induction might suppress collagen production by delaying myofibroblast proliferation and migration.

In non-infarcted sites, excessive collagen accumulation is known to increase myocardial stiffness and to worsen contractile function, contributing to the progression of post-MI remodeling (26). The increased LVEDD and elevated LV end-diastolic pressure in GM-CSF inducer-treated rats may be caused not only by reduced collagen deposition in the infarcted sites but also by increased collagen deposition in the non-infarcted sites. Delayed infarct healing and early LV remodeling induced by GM-CSF might increase wall stress and subsequently promote myocardial remodeling in non-infarcted sites. The GM-

CSF might have a detrimental effect on collagen deposition according to different locations and timing.

We have reported that peak serum C-reactive protein level or peak peripheral monocyte count could be a predictor of adverse LV remodeling and poor long-term outcome after MI. These indices, determined two to three days after MI, could predict long-term LV remodeling, suggesting that an excessive inflammatory response during the early phase of MI could affect the infarct healing process and ventricular structural remodeling (4,27). In our study, romurtide was administered for seven consecutive days after coronary ligation. During this phase, the infarcted myocardium might be most vulnerable to various stimuli including mechanical stress, inflammatory cytokines, and neurohormonal factors. Interventions in the infarct healing process during the early phase of MI might have a great impact on long-term LV remodeling. It has been believed that the use of corticosteroids after MI has a deleterious effect on the infarct healing process and increases the incidence of cardiac rupture or infarct expansion (28). However, a recent meta-analysis demonstrated a possible mortality benefit of administration of corticosteroids for acute MI (29). Inhibition of the excessive inflammatory response, especially monocyte and macrophage activation, during the early phase of MI may be beneficial to prevent LV remodeling.

Study limitations. First, we did not examine the direct effect of GM-CSF on cardiomyocytes. Because GM-CSF administration in cancer patients reduced cardiac contractility, GM-CSF itself might directly influence the infarcted heart (30). Second, GM-CSF promoted collateral growth in patients with chronic coronary artery disease (31). Collateral growth, caused by GM-CSF induction, may influence the infarct healing process. However, the association between collateral growth and LV remodeling was not clarified in our setting. Third, GM-CSF induced the mobilization of bone marrow-derived endothelial progenitor cells for neovascularization (32). Although regeneration therapy for injured myocardium, consisting of myocytes, vessels, and ECM, could be effective for preventing post-MI remodeling, the effect of GM-CSF induction on regeneration of injured myocardium was not examined in this study. The possibility of GM-CSF for myocardial regeneration will be further investigated.

Conclusions. The GM-CSF induction by romurtide resulted in infarct expansion and aggravated LV remodeling. The acute inflammatory response during the early phase of MI could be a potential target for the treatment of patients with MI.

Reprint requests and correspondence: Dr. Toshihisa Anzai, Division of Cardiology, Department of Medicine, Keio University School of Medicine, 35 Shinanomachi, Shinjuku-ku, Tokyo 160-8582, Japan. E-mail: anzai@cpnet.med.keio.ac.jp.

REFERENCES

1. Zardini P, Marino P, Golia G, Anselmi M, Castelli M. Ventricular remodeling and infarct expansion. Am J Cardiol 1993;72:98G–106G.
2. Pfeffer MA, Braunwald E. Ventricular remodeling after myocardial infarction. Experimental observations and clinical implications. Circulation 1990;81:1161–72.
3. Gasson JC. Molecular physiology of granulocyte-macrophage colony-stimulating factor. Blood 1991;77:1131–45.
4. Maekawa Y, Anzai T, Yoshikawa T, et al. Prognostic significance of peripheral monocytosis after reperfused acute myocardial infarction: a possible role for left ventricular remodeling. J Am Coll Cardiol 2002;39:241–6.
5. Parissis JT, Adamopoulos S, Venetsanou KF, et al. Clinical and neurohormonal correlates of circulating granulocyte-macrophage colony-stimulating factor in severe heart failure secondary to ischemic or idiopathic dilated cardiomyopathy. Am J Cardiol 2000;86:707–10, A9–10.
6. Azuma I. Review: inducer of cytokines in vivo: overview of field and romurtide experience. Int J Immunopharmacol 1992;14:487–96.
7. Broudy VC, Kaushansky K, Shoemaker SG, Aggarwal BB, Adamson JW. Muramyl dipeptide induces production of hemopoietic growth factors in vivo by a mechanism independent of tumor necrosis factor. J Immunol 1990;144:3789–94.
8. Ju H, Zhao S, Jassal DS, Dixon IM. Effect of AT1 receptor blockade on cardiac collagen remodeling after myocardial infarction. Cardiovasc Res 1997;35:223–32.
9. Mannisi JA, Weisman HF, Bush DE, Dudeck P, Healy B. Steroid administration after myocardial infarction promotes early infarct expansion: a study in the rat. J Clin Invest 1987;79:1431–9.
10. Bunger MK, Wilsbacher LD, Moran SM, et al. Mop3 is an essential component of the master circadian pacemaker in mammals. Cell 2000;103:1009–17.
11. Stegemann H, Stalder K. Determination of hydroxyproline. Clin Chim Acta 1967;18:267–73.
12. Ashcroft GS, Lei K, Jin W, et al. Secretory leukocyte protease inhibitor mediates non-redundant functions necessary for normal wound healing. Nat Med 2000;6:1147–53.
13. Mori R, Kondo T, Ohshima T, Ishida Y, Mukaida N. Accelerated wound healing in tumor necrosis factor receptor p55-deficient mice with reduced leukocyte infiltration. FASEB J 2002;16:963–74.
14. Buschmann IR, Hoefer IE, van Royen N, et al. GM-CSF: a strong arteriogenic factor acting by amplification of monocyte function. Atherosclerosis 2001;159:343–56.
15. Coxon A, Tang T, Mayadas TN. Cytokine-activated endothelial cells delay neutrophil apoptosis in vitro and in vivo: a role for granulocyte/macrophage colony-stimulating factor. J Exp Med 1999;190:923–34.
16. Rollins BJ, Yoshimura T, Leonard EJ, Pober JS. Cytokine-activated human endothelial cells synthesize and secrete a monocyte chemoattractant, MCP-1/JE. Am J Pathol 1990;136:1229–33.
17. Shyy YJ, Li YS, Kolattukudy PE. Activation of MCP-1 gene expression is mediated through multiple signaling pathways. Biochem Biophys Res Commun 1993;192:693–9.
18. Trueblood NA, Xie Z, Communal C, et al. Exaggerated left ventricular dilation and reduced collagen deposition after myocardial infarction in mice lacking osteopontin. Circ Res 2001;88:1080–7.
19. Jorgensen LN, Agren MS, Madsen SM, et al. Dose-dependent impairment of collagen deposition by topical granulocyte-macrophage colony-stimulating factor in human experimental wounds. Ann Surg 2002;236:684–92.
20. Cleutjens JP, Verluyten MJ, Smiths JF, Daemen MJ. Collagen remodeling after myocardial infarction in the rat heart. Am J Pathol 1995;147:325–38.
21. Lindsey M, Wedin K, Brown MD, et al. Matrix-dependent mechanism of neutrophil-mediated release and activation of matrix metalloproteinase 9 in myocardial ischemia/reperfusion. Circulation 2001;103:2181–7.
22. Dollery CM, McEwan JR, Henney AM. Matrix metalloproteinases and cardiovascular disease. Circ Res 1995;77:863–8.
23. Heymans S, Luttun A, Nuyens D, et al. Inhibition of plasminogen activators or matrix metalloproteinases prevents cardiac rupture but impairs therapeutic angiogenesis and causes cardiac failure. Nat Med 1999;5:1135–42.

24. Creemers E, Cleutjens J, Smits J, et al. Disruption of the plasminogen gene in mice abolishes wound healing after myocardial infarction. Am J Pathol 2000;156:1865–73.
25. Sun Y, Weber KT. Infarct scar: a dynamic tissue. Cardiovasc Res 2000;46:250–6.
26. Weber KT. Extracellular matrix remodeling in heart failure: a role for de novo angiotensin II generation. Circulation 1997;96:4065–82.
27. Anzai T, Yoshikawa T, Shiraki H, et al. C-reactive protein as a predictor of infarct expansion and cardiac rupture after a first Q-wave acute myocardial infarction. Circulation 1997;96:778–84.
28. Roberts R, DeMello V, Sobel BE. Deleterious effects of methylprednisolone in patients with myocardial infarction. Circulation 1976;53: I204–6.
29. Giugliano GR, Giugliano RP, Gibson CM, Kuntz RE. Meta-analysis of corticosteroid treatment in acute myocardial infarction. Am J Cardiol 2003;91:1055–9.
30. Knoops S, Groeneveld AB, Kamp O, Lagrand WK, Hoekman K. Granulocyte-macrophage colony-stimulating factor (GM-CSF) decreases left ventricular function: an echocardiographic study in cancer patients. Cytokine 2001;14:184–7.
31. Seiler C, Pohl T, Wustmann K, et al. Promotion of collateral growth by granulocyte-macrophage colony-stimulating factor in patients with coronary artery disease: a randomized, double-blind, placebo-controlled study. Circulation 2001;104:2012–7.
32. Takahashi T, Kalka C, Masuda H, et al. Ischemia- and cytokine-induced mobilization of bone marrow-derived endothelial progenitor cells for neovascularization. Nat Med 1999;5:434–8.